7 JANUARY 2012 Volume 136 Number 1

AIP | The Journal of Chemical Physics

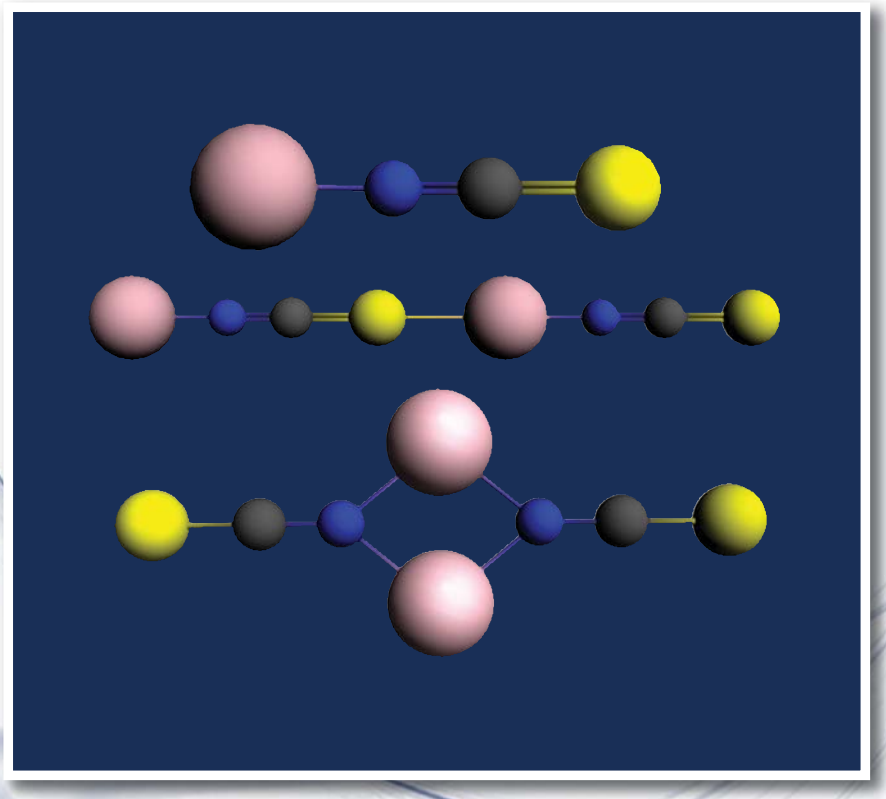

Influence of solute-solvent coordination on
the orientational relaxation of ion assemblies in polar solvents
by M. Ji, R. W. Hartsock, Z. Sung, and K. W. Gaffney

jcp.aip.org

Influence of solute-solvent coordination on the orientational relaxation of ion assemblies in polar solvents

Minbiao Ji, Robert W. Hartsock, Zheng Sung, and Kelly J. Gaffney

Citation: J. Chem. Phys. **136**, 014501 (2012); doi: 10.1063/1.3665140
View online: http://dx.doi.org/10.1063/1.3665140
View Table of Contents: http://jcp.aip.org/resource/1/JCPSA6/v136/i1
Published by the American Institute of Physics.

Influence of solute-solvent coordination on the orientational relaxation of ion assemblies in polar solvents

Minbiao Ji,[1,2,a)] Robert W. Hartsock,[1,3] Zheng Sung,[1] and Kelly J. Gaffney[1,b)]
[1]*PULSE Institute, SLAC National Accelerator Laboratory, Stanford University, Stanford, California 94305, USA*
[2]*Department of Physics, Stanford University, Stanford, California 94305, USA*
[3]*Department of Chemistry, Stanford University, Stanford, California 94305, USA*

(Received 5 August 2011; accepted 10 November 2011; published online 3 January 2012)

We have investigated the rotational dynamics of lithium thiocyanate (LiNCS) dissolved in various polar solvents with time and polarization resolved vibrational spectroscopy. LiNCS forms multiple distinct ionic structures in solution that can be distinguished with the CN stretch vibrational frequency of the different ionic assemblies. By varying the solvent and the LiNCS concentration, the number and type of ionic structures present in solution can be controlled. Control of the ionic structure provides control over the volume, shape, and dipole moment of the solute, critical parameters for hydrodynamic and dielectric continuum models of friction. The use of solutes with sizes comparable to or smaller than the solvent molecules also helps amplify the sensitivity of the measurement to the short-ranged solute-solvent interaction. The measured orientational relaxation dynamics show many clear and distinct deviations from simple hydrodynamic behavior. All ionic structures in all solvents exhibit multi-exponential relaxation dynamics that do not scale with the solute volume. For Lewis base solvents such as benzonitrile, dimethyl carbonate, and ethyl acetate, the observed dynamics strongly show the effect of solute-solvent complex formation. For the weak Lewis base solvent nitromethane, we see no evidence for solute-solvent complex formation, but still see strong deviation from the predictions of simple hydrodynamic theory. © *2012 American Institute of Physics*. [doi:10.1063/1.3665140]

I. INTRODUCTION

Ultrafast laser spectroscopy has been utilized to experimentally investigate solvation dynamics with the express goal of investigating the validity and applicability of theoretical descriptions of solvation dynamics. The time dependent evolution of the spectral[1–4] and orientational[5–7] memory of an electronically excited chromophore embedded in a solvent has provided the dominant means of investigating the dynamics of solvation. While these measurements have clearly demonstrated that the environment, be it a bulk solvent,[1,3,8] ionic liquid,[9] glass,[10] protein, [11] interface,[12] reverse micelle,[13] or cluster[14] greatly influences the dynamics of the solute-solvent interaction, the identification of which physical properties of the solute-solvent interaction dominate and under what circumstances they dominate generally remains undetermined.

Continuum models have proven to be surprisingly successful in describing the general attributes of solvation dynamics,[1,4] despite many attempts to identify the molecular scale origins of solvation dynamics. For the case of orientational relaxation, the Debye-Stokes-Einstein description of hydrodynamic friction has often been able to effectively describe orientational relaxation in solution.[6] Thorough analysis of experimental data does, however, identify important and persistent deviations from simple hydrodynamic behavior.[6] The challenge in addressing these exceptions derives in large part from the enormous range of potential explanations. Critical influences on the predicted dynamics include choosing between slip or stick boundary conditions,[6,15,16] the presence of long-lived solute-solvent complex formation,[17] the importance of the solute-solvent size ratio,[5,6,18–20] and long-ranged electrostatic effects generally characterized as dielectric friction.[6,7,21] Disentangling these various influences proves difficult, because rarely can these distinct effects be isolated experimentally. For instance, changing the solvent viscosity rarely leaves the solvent size or dielectric properties unchanged. The utilization of dye molecules and specifically the electronic excitations of dyes to probe the molecular scale interaction of solute and solvent also presents a key limitation, since the size of the dye usually exceeds the solvent size significantly and leads to an effective spatial averaging that suppresses the sensitivity of the measurement to short-ranged solute-solvent interactions.

Simple continuum models, such as the Debye-Stokes-Einstein model, predict single exponential relaxation dynamics, but complex relaxation dynamics does not guarantee deviation from continuum dynamics. In general, the viscous or dielectric drag depends upon the frequency of the motion being impeded even in the long wavelength limit. A frequency dependent viscosity or dielectric function will lead to multi-exponential dynamics without the need for spatial heterogeneity in the dynamics.

We have chosen to address some of the limitations and challenges of prior studies by using time and polarization

a)Present address: Department of Chemistry and Chemical Biology, Harvard University, Cambridge, Massachusetts 02138, USA.
b)Electronic mail: kgaffney@slac.stanford.edu.

resolved vibrational spectroscopy.[22] In prior studies of the hydroxyl stretch of water in aqueous sodium perchlorate solution, we demonstrated the ability of time- and polarization-resolved vibrational spectroscopy determine the mechanism for water rotation.[23,24] Here we have used the technique to study the rotational dynamics of lithium thiocyanate (LiNCS) dissolved in various polar solvents. LiNCS forms several types of ionic assemblies in solution depending on the LiNCS concentration and the properties of the solvent, with the CN-stretch frequency providing a sensitive marker of the distinct ionic structures[25–29] and an excellent probe of orientational dynamics because of the long vibrational excited state lifetime.[24,28–31] In strong polar solvents with Lewis base electron donating properties, such as dimethyl sulfoxide and acetonitrile, LiNCS exists predominantly as free ions at low ionic concentration and ion pairs at high concentration. In strongly polar solvents with poor electron donating properties, such as nitromethane, ion-pair dimers dominate. Ion-pair dimers also dominate in moderate to weakly polar solvents with strong electron donating properties, such as dimethyl carbonate, ethyl acetate, and benzonitrile.

These LiNCS assemblies have many properties that make them excellent for investigating the influence of non-continuum solvation effects on orientational dynamics. The solvent and LiNCS concentration can be chosen so that structurally distinct ionic assemblies coexist at equilibrium. This allows us to vary the ratio of the solute-to-solvent volume without having to change the solvent or the nature of the short-ranged solute-solvent interaction. These distinct ionic assemblies also have distinct electrostatic charge distributions, allowing the orientational dynamics to be measured for structures with a net charge, a charge dipole, and a charge quadrupole structure. This variation in charge distribution can also be achieved without significant variation in the shape and volume of the ionic structure. This allows the influence of electrostatic effects and solute-solvent complex formation to be isolated from those of solute size and shape. Lastly, the simplicity of the chemical systems studied and the small perturbation of the solute-solvent interaction generated by vibrational excitation makes the measurements amenable to molecular dynamics simulations and provides the opportunity for a detailed molecular understanding of the observed phenomena.

II. EXPERIMENTAL AND THEORETICAL METHODS

We generate 800 nm pulses with a Ti:sapphire oscillator (MTS, KM Labs) and regenerative amplifier (Spitfire, Spectra-Physics) laser system at 1 kHz. The 800 nm pulses with 45 fs duration and ~1 mJ per pulse were used to pump an optical parametric amplifier (OPA800CF, Spectra-Physics) to produce near-IR pulses at ~1.4 and ~1.9 μm which were utilized to generate mid-IR pulses at 2050 cm^{-1} in a 0.5 mm thick $AgGaS_2$ crystal by difference frequency generation. The power spectrum of the mid-IR pulses had a Gaussian envelope with a ~270 cm^{-1} bandwidth (full width at half-maximum). We measured the pulse chirp with frequency-resolved optical gating measurements in a transient grating geometry. We used CaF_2 plates with different thicknesses to compensate for the linear dispersion introduced by other dielectric materials in the setup, particularly a Ge Brewster plate. This setup produced transform-limited mid-IR pulses with pulse durations of ~65 fs at the sample and pulse energies of 2–4 μJ.

For the polarization resolved pump-probe measurements, we split the mid-IR pulses into pump and probe beams with a relative intensity of 9:1. We focus these beams onto the sample with an off-axis parabolic mirror, generating a roughly 50 μm squared spot size. We control the relative timing of the pump and probe with computer controlled translation stage. We collimate the probe beam after the sample and use a grating spectrometer (iHR320, Horiba) to disperse the probe beam with a grating onto a 32 × 2 element mercury-cadmium-telluride (MCT) array detector with high-speed data acquisition electronics (FPAS-6416-D, Infrared Systems Development Corp.). We use wire grid polarizers to control the polarization of the pump and probe pulses. We placed them in the pump and probe beam before the sample and in front of the entrance slit on the spectrometer.

We utilized Amsterdam Density Function to calculate gas phase structures and vibrational absorption spectra for a variety of LiNCS ionic structures.[32] We utilized the Vosko-Wilk-Nusair (VWN) local density functional in conjunction with the triple-ζ polarized (TZP) basis set without any frozen cores when optimizing the geometry of the dimer structures. The same settings were used when calculating the infrared absorption spectra analytically. Scalar relativistic effects were left on during the calculations. We pre-optimized all calculated structures using the molecular mechanics approach.

Detailed preparation procedures for LiNCS ion pair and dimer equilibrium solutions have been described elsewhere.[27,28] We purchased benzonitrile (BN), nitromethane ($MeNO_2$), dimethyl carbonate (DMC), ethyl acetate (EtAct), and LiNCS hydrate from Sigma-Aldrich. We used the solvents as received, and dried the $LiSCN \cdot xH_2O$ with a literature procedure.[27] We prepared the solutions by dissolving LiNCS in each solvent and then centrifuged the solutions for 15 min to precipitate the suspended particles. We sealed the sample between two CaF_2 windows spaced by a 3 μm PET spacer to generate a maximum absorbance of roughly 0.4 for the 1.2 M LiNCS solutions. We performed the time resolved vibrational measurements at 22°C over a spectral range from 1984 to 2110 cm^{-1} with a resolution of 4 cm^{-1}.

III. RESULTS

A. Vibrational spectroscopy

Figure 1 shows the FTIR spectra in the spectral region of the CN stretch of NCS^- for a 1.2 M LiNCS solution in $MeNO_2$. Extensive experimental studies using FTIR, Raman, and NMR spectroscopy have been used to determine the nuclear structure associated with each CN-stretch peak in the FTIR spectra.[25,33–36] The peak at 2073 cm^{-1} corresponds to the CN stretch absorption of the ion pair,[25,36] the peak at 2042 cm^{-1} corresponds to the CN stretch absorption of an ion-pair dimer with a quadrupole charge distribution (Q-dimer),[35,36] and the small blueshifted peak in $MeNO_2$ at 2102 cm^{-1} corresponds to the thiocyanate anion coordinating Li^+ cations

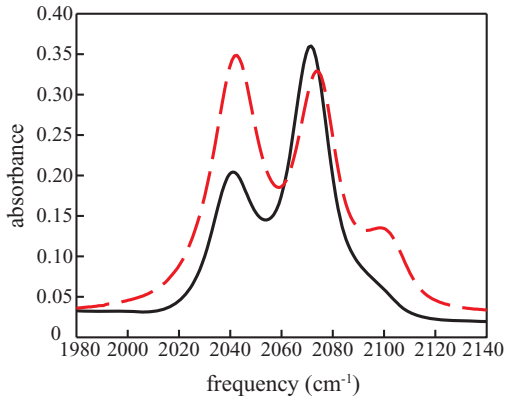

FIG. 1. FTIR spectra of 1.2 M LiNCS in benzonitrile (BN: solid black line) and nitromethane ($MeNO_2$: dashed red line). The peak at ~2040 cm^{-1} corresponds to an ion-pair dimer structure with a quadrupole charge distribution (Q-dimer), the peak at ~2070 cm^{-1} corresponds to the LiNCS ion pair, and the peak at ~2100 cm^{-1} corresponds to the NCS^- in a linear ion-pair dimer (L-dimer) that is coordinating two Li^+ cations, one with the N atom and the other with the S atom.

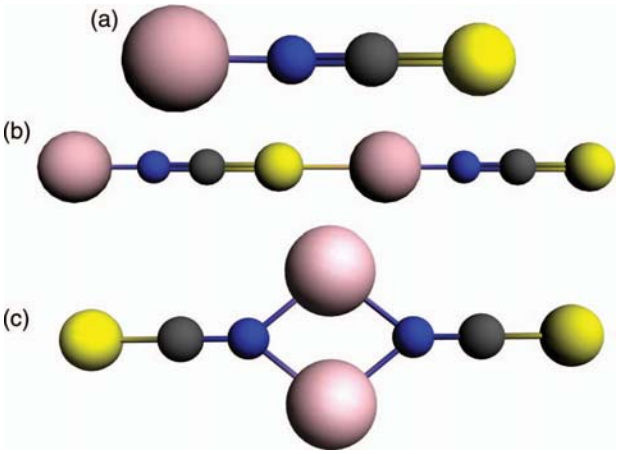

FIG. 2. Calculated gas phase structures for the (a) ion pair, (b) linear ion-pair dimer (L-dimer) structure, and (c) ion-pair dimer with a quadrupole charge distribution (Q-dimer). The following atomic color scheme are used: Li, mauve; N, blue; C, black; and S, yellow. The size of the spheres do not reflect the electronic charge density.

with both the sulfur and nitrogen in a linear ion-pair dimer (L-dimer).[34] LiNCS concentration-dependent FTIR spectra in benzonitrile can be found in the supplementary material.[42]

We have also performed a series of quantum chemical calculations to support these assignments. We used the VWN local density functional to optimize the geometry of the ion pair and the Q-dimer and L-dimer structures. The Q-dimer structure appears to be the lowest energy dimer structure in the gas phase. Using a linear symmetry constraint, we calculated the structure and vibrational spectrum of the L-dimer, but relaxation of the symmetry constraint leads to spontaneously conversion to the quadrupolar dimer structure. The lithium thiocyanate ion pair has CN-stretch frequencies of 2071 cm^{-1}. The Q-dimer contained two modes of vibration dominated by CN-stretching, a symmetric (2045 cm^{-1}) Raman active vibration and an anti-symmetric (2018 cm^{-1}) IR active vibration. The two CN-stretch vibrations of the L-dimer happen to be strongly localized to individual CN moieties. These vibrations occur at 2077 cm^{-1} for the thiocyanate nitrogen coordinating one Li^+ and 2126 cm^{-1} for the thiocyanate that nitrogen and sulfur coordinates two Li^+. These calculation results parallel the findings of prior theoretical studies using *ab initio*[37] and semi-empirical methods.[38] The different ionic structures appear in Figure 2 and the calculated and experimental CN stretch frequencies appear in Table I.

The mid-IR spectroscopy of the dimer structures presents additional complications for the interpretation of the orientational relaxation dynamics because each dimer has two CN-stretch chromophores. In the case of the Q-dimer structure, the presence of a center of inversion eliminates this complication because only the asymmetric CN-stretch absorbs in the mid-IR. For the L-dimer, the two CN-stretches will both be IR active and generate two CN-stretch absorptions in the mid-IR absorption spectrum. For solutions possessing all three ionic structures—ion pairs, Q-dimers, and L-dimers—quantum chemical calculations predict four CN-stretch absorption peaks, but we only observe three distinct peaks experimentally. The theoretical calculations indicate that one of the L-dimer absorptions will overlap with the CN-stretch of the ion pair, though the roughly 20 cm^{-1} accuracy of the calculated frequencies leaves uncertainty about the spectral positions of the various ionic structures. This means that for the $MeNO_2$ solution, the peak nominally associated with the ion pair structure could also have a contribution from one of the L-dimer CN-stretch absorptions. This should have minimal effect on the dynamics observed in BN, DMC, and EtAct solutions because of the very small L-dimer concentration.

Since long-lived solvent-solute complex formation can have a significant impact on the rotational dynamics of the chromophore, we have also used vibrational spectroscopy to characterize the solute-solvent interaction. As can be seen in Figure 3(a), complex formation between BN and Li^+ leads to a significant shift in the CN stretch of BN. Previous measurements of the spectral diffusion and assembly dynamics strongly indicate that electron pair donating solvents such as BN, DMC, and EtAct form long-lived coordination complexes with Li^+ cations in the ionic assemblies.[31] As can be seen in Figure 3(b), the symmetric and asymmetric stretches of the nitro group of $MeNO_2$ shows no evidence of complex formation with Li^+, strongly indicating that the nitro group at most forms weak and short-lived complexes with lithium cations. These different interactions between the solute and solvent lead to very different orientational relaxation dynamics, as will be addressed in Sec. III B.

TABLE I. Experimental and calculated absorption peak frequencies, and van der Waals volumes[40] of LiNCS ion pair, quadrupole ion-pair dimer (Q-dimer), and linear ion-pair dimer (L-dimer) in $MeNO_2$.

	Experimental frequencies (cm^{-1})	Calculated frequencies (cm^{-1})	Volume (Å^3)
Pair	2073.6	2071	45
Q-dimer	2041.6	2018	92
L-dimer	2099	2126	94

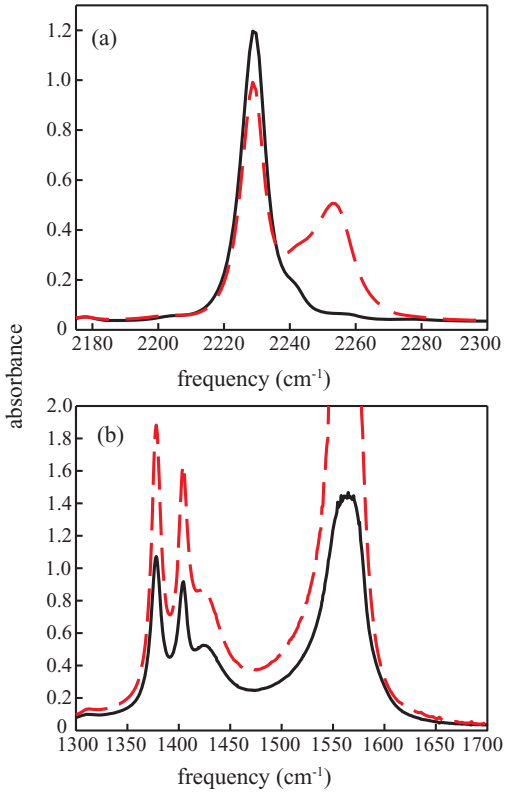

FIG. 3. (a) FTIR spectra of benzonitrile (BN: solid black line) and 1.2 M LiNCS in benzonitrile in the region of the CN-stretch of BN (dashed red line). Note the appearance of a blueshifted CN stretch due to direct coordination of Li^+ cations by the cyano-group on BN. (b) FTIR spectra of nitromethane ($MeNO_2$: solid black line) and 1.2 M LiNCS in nitromethane (dashed red line) in the region of the symmetric and anti-symmetric nitro-group stretching vibrations. We collected the pure solvent spectra with a 2 μm path length cell and the ionic solution spectra with a 6 μm path length cell. LiNCS causes a slight broadening of the symmetric and anti-symmetric nitro-group stretching vibrations, but we see no spectral evidence for Li^+ coordination by $MeNO_2$.

B. Pump-probe measurements of orientational relaxation

In mid-IR pump-probe experiments, a pump pulse excites the first vibrational excited state ($\upsilon = 1$), and we subsequently follow the time evolution of the vibrational excitation with a time-delayed probe pulse. The pump pulse leads to a ground state bleach and stimulated emission at the frequency of the $\upsilon = 0 \rightarrow 1$ transition and excited state absorption at the anharmonically shifted $\upsilon = 1 \rightarrow 2$ transition. The parallel, $S_{\parallel}(t)$, and perpendicular, $S_{\perp}(t)$, components of the pump-probe signals at each frequency are measured with the polarization of the pump beam parallel and perpendicular to the probe beam, respectively. These signals were used to obtain the vibrational population relaxation,

$$P(t) = S_{\parallel}(t) + 2S_{\perp}(t), \tag{1}$$

and the orientational anisotropy,

$$r(t) = \frac{S_{\parallel}(t) - S_{\perp}(t)}{S_{\parallel}(t) + 2S_{\perp}(t)} = \frac{2}{5}C_{or}(t). \tag{2}$$

The population relaxation dynamics have been published previously.[28,31] The orientational anisotropy, $r(t)$, measures the orientational relaxation dynamics of the CN stretch transition dipole as reflected by the second-order Legendre polynomial of the transition dipole correlation function, $C_2 = \langle P_2[\boldsymbol{\mu}(t) \cdot \boldsymbol{\mu}(0)]\rangle$, while the population relaxation, $P(t)$, measures the decay of the vibrationally excited molecules.

The presence of two or more distinct ionic structures generates multiple CN stretch transitions in the absorption spectrum and may lead to overlapping signals resulting from the $\upsilon = 0 \rightarrow 1$ transition of one chemical species and the $\upsilon = 1 \rightarrow 2$ transition of another. For the BN, DMC, and EtAct solutions, we avoid this complication by using the $\upsilon = 1 \rightarrow 2$ transition to study the dynamics of the quadrupolar ion-pair dimer and the $\upsilon = 0 \rightarrow 1$ transition for the ion pair since these signals reside at the spectral extremes of the measurement and insure no overlapping signal. We have used the ion pair $\upsilon = 0 \rightarrow 1$ response at 2071 cm^{-1}, the Q-dimer $\upsilon = 1 \rightarrow 2$ response at 2019 cm^{-1}, and the L-dimer $\upsilon = 0 \rightarrow 1$ response at 2105 cm^{-1} to measure orientational relaxation dynamics.

The $MeNO_2$ solution presents an additional complication, because we only resolve one of the two CN-stretch absorptions of the L-dimer structure. The theoretical calculations predict that the terminal thiocyanate coordinating a single Li^+ in the L-dimer has an absorption frequency experimentally indistinguishable from the ion pair. This could indicate that both the L-dimer and the ion pair contribute to the dynamics measured at roughly 2071 cm^{-1}. If we use similar absorption cross-sections for each thiocyanate in the L-dimer having a similar absorption cross-section to the ion pair, as predicted by theory, the thiocyanate in the linear dimer contributes roughly 10% of the signal for $MeNO_2$ and an insignificant amount of the signal for BN, DMC, and EtAct. We would like to emphasize that these effects will be insignificant for BN, DMC, and EtAct because the L-dimer population is much smaller and all the ionic species have similar orientational relaxation dynamics. For $MeNO_2$, these effects may subtly suppress the distinctions between the orientational relaxation of the different ionic assemblies.

Figure 4 shows the anisotropy dynamics for each stable ionic configuration in the BN and $MeNO_2$ solutions. The anisotropy data for the DMC and EtAct solutions can be found in the supplementary material.[42] All ionic structures in all the solvents studied exhibit multi-exponential orientational relaxation dynamics that we have fit with a tri-exponential function. Figure 4 also shows the best fit for BN and $MeNO_2$. The extracted time constants and amplitudes for all ionic structures in the studied solvents appear in Table II. Before discussing the significance of these measurements, the limitations of the data analysis should be mentioned. As demonstrated in previous 2DIR spectroscopy studies of chemical exchange in these solutions, chemical inter-conversion between the distinct ionic species occurs on a time scale similar to the orientational relaxation of the ionic assemblies.[31] Since pump-probe spectroscopy measures the contribution of all molecules that absorb at a given frequency, independent of the absorber prior spectral history, we average the orientational dynamics of vibrationally excited thiocyanates that have resided in a single ionic configuration with those that have undergone a chemical exchange during the

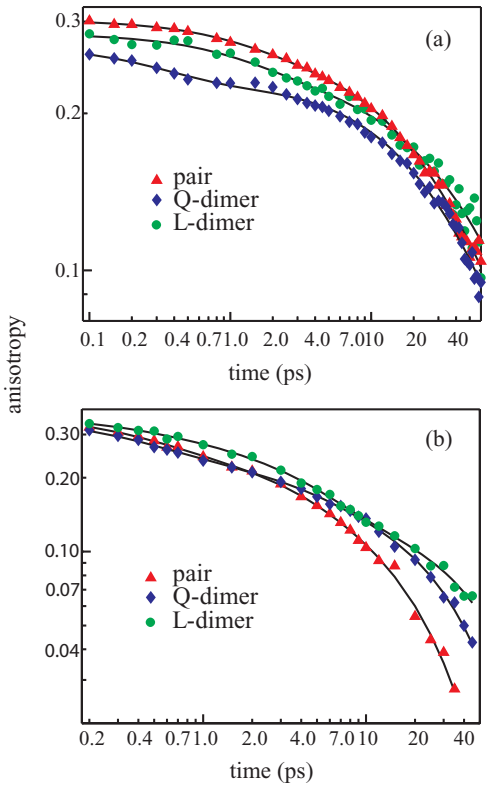

FIG. 4. Logarithmic plot of the time resolved anisotropy for 1.2 M LiNCS in (a) benzonitrile (BN) and (b) nitromethane ($MeNO_2$) measured with polarization selective vibrational pump-probe measurements of the orientational CN stretch of NCS^- in the ion pair, Q-dimer, and L-dimer. Note the different time axes for (a) and (b). The solid black lines show the fit of each data set to a tri-exponential decay. The rotational relaxation time constants and amplitudes extracted from the tri-exponential fits can be found in Table II.

pump-probe time delay. As demonstrated by these previous 2DIR spectroscopy studies, the excited molecules that have resided in a single ionic structure dominate the signal for the first 40 ps. For time delays longer than 40 ps, the chemically exchanged populations will no longer be negligible. The exchanged populations still only have a minor effect on the majority of the measured dynamics because the cross-peaks lose orientational memory with a rate equal to the average of the orientational relaxation rates of the two ionic species undergoing chemical exchange. For these reasons, chemical exchange only has a significant effect of the observed anisotropy measurements for time delays longer than the chemical exchange rate and when the distinct ionic structures have significantly different orientational relaxation dynamics.

Inspection of the initial orientational relaxation for the Q-dimer species in BN, DMC, and EtAct, all show a small amplitude oscillation. This oscillation does not occur for the Q-dimer in $MeNO_2$ or for the ion pair or L-dimer in any solution. This strongly damped oscillation in the time dependent anisotropy can be found in Figure 5 for the Q-dimer in BN and DMC. The fit to the experimental data gives an oscillation frequency of roughly 15–20 cm^{-1} for both solutions. The coherent oscillation in the anisotropy indicates that CN-stretch excitation leads to impulsive excitation of vibrations or librations of the Q-dimer. The density functional calculations predict the in- and out-of-plane wag of the Q-dimer to modulate the orientation of the CN groups and a frequency of roughly 30 cm^{-1}. Given the low frequency of the coherently excited motion, compared to the CN-stretch frequency, strongly anharmonic coupling between the CN stretch and the Q-dimer in- and out-of-plane wagging motions could also produce the observed signal.

TABLE II. Parameters extracted from the fit of the anisotropy data to a bi-exponential decay function: $r(t) = A_1 e^{-t/\tau_{or1}} + A_2 e^{-t/\tau_{or2}} + A_3 e^{-t/\tau_{or3}}$. The amplitudes have errors of 10% or less.

Solvents	Ionic species	A_1	τ_{or1}(ps)	A_2	τ_{or2}(ps)	A_3	τ_{or3}(ps)
BN	Pair	0.04	1.0 ± 0.5	0.22	15 ± 3	0.17	120 ± 20
	Q-dimer	0.04	0.2 ± 0.1	0.20	9 ± 3	0.19	90 ± 10
	L-dimer	0.03	1.5 ± 0.5	0.04	10 ± 5	0.21	120 ± 40
$MeNO_2$	Pair	0.10	0.45 ± 0.15	0.11	3.5 ± 1.5	0.16	20 ± 3
	Q-dimer	0.10	0.4 ± 0.1	0.08	4 ± 2	0.17	34 ± 5
	L-dimer	0.05	0.6 ± 0.2	0.16	4 ± 1	0.15	50 ± 5
DMC	Pair	0.10	0.5 ± 0.1	0.10	7 ± 2	0.17	47 ± 5
	Q-dimer	0.10	0.4 ± 0.1	0.04	7 ± 3	0.18	54 ± 6
EtAct	Pair	0.09	0.3 ± 0.1	0.10	4 ± 2	0.20	36 ± 4
	Q-dimer	0.11	0.4 ± 0.1	0.06	5 ± 2	0.18	49 ± 6

IV. DISCUSSION

The Debye-Stokes-Einstein theory of hydrodynamic friction predicts the exponential decay of the second-order Legendre polynomial of the transition dipole correlation function, $C_2 = \langle P_2[\boldsymbol{\mu}(t) \cdot \boldsymbol{\mu}(0)]\rangle$, with a rotational time constant,

$$\tau = \frac{V_P f \eta}{k_B T} C, \tag{3}$$

where V_P represents the probe volume, f represents a scaling factor that accounts for the shape of the solute, η represents the shear viscosity of the solution, and C can be considered as a coupling parameter[16] that corrects for deviations from simple hydrodynamic rotational friction.

The observed anisotropy decays deviate substantially from those predicted by the Debye-Stokes-Einstein theory.

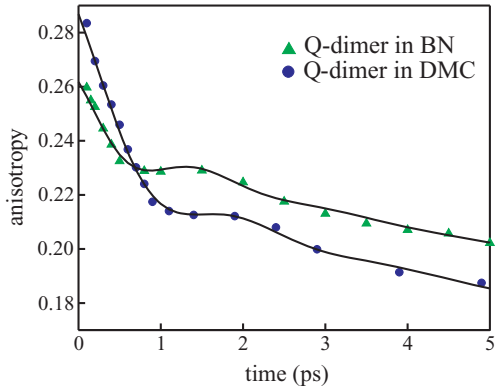

FIG. 5. Early time decay of the anisotropy for the Q-dimer in benzonitrile (BN) and dimethyl carbonate (DMC). The time dependent decay of the anisotropy shows a strongly damped oscillation, with a frequency of ~18 cm^{-1} for BN and ~15 cm^{-1} for DMC.

We will highlight the deviations and then systematically discuss the various solute and solvent properties that could potentially explain the deviations. All ionic structures in all solvents show multi-exponential orientational relaxation dynamics. The amplitude of the orientational dynamics captured by the tri-exponential fit to the experimental data does not equal 0.4 at zero time delay, indicating that an additional sub-100 fs orientational relaxation also occurs that we do not resolved experimentally for all ionic structures in all solvents.

The tri-exponential decay does not result from multiple moments of inertia for the distinct ionic structures. For the ion pair and the L-dimer structures with their CN-stretch transition dipole moments oriented parallel to the high symmetric axis, only one moment of inertia leads to the re-orientation of the transition dipole moment. For the Q-dimer structure, the transition dipole moment also lies parallel to the high symmetry axis of the assembly. The displacement of the Li+ cations from the high symmetry axis leads to two moments of inertia for the Q-dimer that reorient the CN-stretch transition dipole moment, but they only differ 1%, making the structure effectively linear. Given the high symmetry of the ionic structures, the appearance of multi-exponential dynamics clearly demonstrates a strong deviation from the simple hydrodynamics expected for an oblate spheroid with the transition dipole parallel to the high symmetry axis.[39]

The multi-exponential relaxation dynamics could be a consequence of homogeneous, but complex, orientational relaxation for each distinct ionic assembly or simple, but heterogeneous, orientational relaxation dynamics for a complex distribution of conformations within each distinct ionic structure. A prior study of the spectral relaxation dynamics of LiNCS ion assemblies in these four solvents[31] shows correlation between the spectral relaxation dynamics and the orientational relaxation dynamics. This correlation could indicate that the orientation of the solute, as opposed to solely the solvent, represents an important source of spectral memory loss, or the correlation could indicate that dissociation of certain solute-solvent conformations dictate the rate of spectral and orientational relaxation. The latter scenario could lead to appreciable heterogeneity in the orientational dynamics. We will now assess the validity of assigning the multi-exponential orientational dynamics to homogeneous, frequency-dependent frictional forces.

For a frequency dependent visco-elastic friction, the low frequency viscosity would be analogous to the viscosity used in the Debye-Stokes-Einstein equation. This would indicate that the slowest orientational relaxation time could be described with the Debye-Stokes-Einstein equation and lead to a slowest relaxation time constant proportional to the solute volume. But we see strong deviations from linear scaling between the orientational relaxation times and the calculated van der Waals volumes[40] of the solutes, V_P, of 45 Å^3 for the ion pair, 92 Å^3 for the Q-dimer, and 94 Å^3 for the L-dimer. Multiple explanations could potentially explain the nonlinear solute volume dependence of the slow orientational relaxation time. The study of Horng *et al*. associated deviations from hydrodynamic continuum theory primarily with systems with small solute to solvent volume ratios, $\rho = \frac{V_P}{V_s}$.[5,6,19,20] Unsurprisingly, the validity of a hydrodynamic continuum description of the solvent improves greatly when the volume of the solute, V_P, being interrogated experimentally significantly exceeds the volume of the solvent, V_S.[6,19,20] Additionally, Hu and Zwanzig postulated that for small solutes, slip boundary conditions provide a more physically reasonable description of the solute-solvent interaction, where the eccentricity of the spheroid determines the magnitude of the deviation from simple hydrodynamics with stick boundary conditions.[15] The models of Gierer and Wirtz[20] and Dote *et al.*,[19] both predict the orientational relaxation time constant to have a super-linear increase with increasing solute volume V_P when $\rho = (V_P/V_S) \leq 1$. Alternatively, Hu and Zwanzig predict the shape of the spheroid, not just the volume, must be considered, with reductions in spheroidal eccentricity leading to reductions in the orientational relaxation time constant.[15]

For the Gierer and Wirtz and the Dote, Kivelson, and Schwartz models, the relaxation time decreases faster than the solute volume decreases for $\rho \leq 1$, while Hu and Zwanzig effectively predict that the scaling factor, fC will decrease independent of solute volume as the solute becomes more spherical. While these distinct models provide distinct predictions for our particular set of measurements, they predict the same trend since the variation in the ionic volumes (L-dimer > Q-dimer > ion pair) and the ionic spheroid eccentricities (L-dimer > Q-dimer > ion pair) have the same trends. We measure the orientational relaxation as a function of solute size and shape for a fixed solvent size and viscosity. Given the factor of two difference in V_P between the ion pair and Q-dimer, the Debye-Stokes-Einstein model predicts the Q-dimer rotational relaxation time, $\tau^{(Q)}$, to be roughly twice that of the ion pair, $\tau^{(P)}$. The theories of Gierer and Wirtz and Dote, Kivelson, and Schwartz predict more than a factor of two increase in rotational time constant, $(\tau^{(Q)}/\tau^{(P)}) > 2$, because of the increase in ρ, while Hu and Zwanzig also predict $(\tau^{(Q)}/\tau^{(P)}) > 2$ because of the more elongated shape of the Q-dimer. For the strong electron donating solvents, our experimental measurements have the opposite trend, with $(\tau^{(Q)}/\tau^{(P)}) \ll 2$. The orientational relaxation in $MeNO_2$ varies more with ionic structure than in the Lewis base solvents, but still does not conform to any of the above theoretical models. Most prominently, the two dimer structures having effectively the same van der Waals volume and similar spheroid eccentricities, but the L-dimer relaxation time exceeds that of the Q-dimer by a factor of 1.5.

These observations clearly indicate that continuum and solvent free volume effects resulting from the molecularity of the solvent cannot explain the observed dynamics. The strong deviation from hydrodynamic and quasi-molecular hydrodynamic models in the strongly coordinating solvents BN, DMC, and EtAct would appear to result from long-lived solute-solvent complexes, but this cannot explain the observed dynamics in the weakly coordinating $MeNO_2$. The spectra in Figure 3 support this interpretation, with the CN stretch of BN showing strong complex formation with Li^+ in Figure 3(a) and the nitro-stretch of $MeNO_2$ showing no evidence of complex formation with Li^+ in Figure 3(b). For the Lewis base solvents, if the solute-solvent complex remains associated for durations longer than the orientational relaxation, the slow component of the orientational dynamics could be

consistent with hydrodynamic theory once the shape and volume of the full solute-solvent complex has been determined. This cannot, however, explain the slow orientational dynamics observed in $MeNO_2$ where solute-solvent complexes do not form. Dielectric friction provides an alternative potential explanation for the observed dynamics in $MeNO_2$, a hypothesis we intend to pursue in future measurements.

V. CLOSING REMARKS

Continuum models have proven to be surprisingly successful in describing the general attributes of solute solvation and orientational relaxation dynamics, despite many attempts to identify the molecular scale origins of solvation dynamics. To amplify the molecularity of the solute-solvent interaction, we have investigated the rotational dynamics of LiNCS dissolved in various polar solvents with time and polarization resolved vibrational spectroscopy. LiNCS forms distinct ionic structures with variable solute volume and solute dipole moment. These measured orientational relaxation dynamics show many clear and distinct deviations from simple hydrodynamic behavior. All solutes in all solvents exhibit multi-exponential relaxation dynamics that do not scale with the solute volume. For Lewis base solvents such as benzonitrile, dimethyl carbonate, and ethyl acetate, the observed dynamics strongly show the effect of solute-solvent complex formation. For the weak Lewis base solvent nitromethane, we see no evidence for solute-solvent complex formation, but still see strong deviation from the predictions of simple hydrodynamic theory. Preliminary analysis indicates dielectric friction has an influence on the orientational dynamics.

Our analysis remains largely preliminary but indicates three central questions warrant further investigation. How does solute-solvent complex formation influence solvation and orientational relaxation dynamics of LiNCS ionic assemblies in strongly coordinating solvents? How does dielectric friction influence the orientational relaxation dynamics of LiNCS ionic assemblies in weakly coordinating solvents? Do the multi-exponential orientational dynamics result from a heterogeneous distribution of ionic structures with simple orientational dynamics or a homogeneous distribution of ionic structures with complex orientational dynamics? Addressing the influence of dielectric friction in weakly coordinating solvents would benefit from measurements of additional solvents, while determination the extent of dynamical heterogeneity requires the measurement of higher-order orientational correlation functions than the two-time orientational correlation function measured with polarization resolved pump-probe spectroscopy.[41] We intend to investigate the potential influence of dynamical heterogeneity with polarization resolved fifth-order nonlinear optical spectroscopy, a potentially powerful method for assessing dynamical heterogeneity.

ACKNOWLEDGMENTS

This research is supported through the PULSE Institute at SLAC National Accelerator Laboratory by the U.S. Department of Energy (DOE), Office of Basic Energy Sciences.

[1] B. Bagchi and R. Biswas, Adv. Chem. Phys. **109**, 207 (1999).
[2] E. A. Carter and J. T. Hynes, J. Chem. Phys. **94**, 5961 (1991); G. R. Fleming and M. H. Cho, Annu. Rev. Phys. Chem. **47**, 109 (1996).
[3] M. L. Horng, J. A. Gardecki, A. Papazyan, and M. Maroncelli, J. Phys. Chem. **99**, 17311 (1995).
[4] M. Maroncelli, J. Mol. Liq. **57**, 1 (1993); J. D. Simon, Acc. Chem. Res. **21**, 128 (1988).
[5] D. Ben-Amotz and J. M. Drake, J. Chem. Phys. **89**, 1019 (1988).
[6] M. L. Horng, J. A. Gardecki, and M. Maroncelli, J. Phys. Chem. A **101**, 1030 (1997).
[7] R. S. Hartman and D. H. Waldeck, J. Phys. Chem. **98**, 1386 (1994).
[8] E. W. Castner and M. Maroncelli, J. Mol. Liq. **77**, 1 (1998).
[9] R. Karmakar and A. Samanta, J. Phys. Chem. A **106**, 4447 (2002).
[10] L. R. Narasimhan, K. A. Littau, D. W. Pack, Y. S. Bai, A. Elschner, and M. D. Fayer, Chem. Rev. **90**, 439 (1990).
[11] D. P. Zhong, S. K. Pal, and A. H. Zewail, Chem. Phys. Lett. **503**, 1 (2011); P. Abbyad, W. Childs, X. H. Shi, and S. G. Boxer, Proc. Natl. Acad. Sci. U.S.A. **104**, 20189 (2007).
[12] K. B. Eisenthal, Chem. Rev. **96**, 1343 (1996); S. H. Liu, A. D. Miller, K. J. Gaffney, P. Szymanski, S. Garrett-Roe, I. Bezel, and C. B. Harris, J. Phys. Chem. B **106**, 12908 (2002); A. D. Miller, I. Bezel, K. J. Gaffney, S. Garrett-Roe, S. H. Liu, P. Szymanski, and C. B. Harris, Science **297**, 1163 (2002).
[13] N. E. Levinger and L. A. Swafford, Annu. Rev. Phys. Chem. **60**, 385 (2009).
[14] L. Lehr, M. T. Zanni, C. Frischkorn, R. Weinkauf, and D. M. Neumark, Science **284**, 635 (1999).
[15] C. M. Hu and R. Zwanzig, J. Chem. Phys. **60**, 4354 (1974).
[16] D. Kivelson, in *Rotational Dynamics of Small and Macromolecules*, edited by T. Dorfmuller and R. Pecora (Springer-Verlag, Berlin, 1987), vol. 293, p. 1.
[17] M. G. Kurnikova, N. Balabai, D. H. Waldeck, and R. D. Coalson, J. Am. Chem. Soc. **120**, 6121 (1998).
[18] M. I. Sluch, M. M. Somoza, and M. A. Berg, J. Phys. Chem. B **106**, 7385 (2002).
[19] J. Dote, D. Kivelson, and R. N. Schwartz, J. Phys. Chem. **85**, 2169 (1981).
[20] A. Gierer and K. Wirtz, Z. Naturforsch. **8**, 532 (1953).
[21] J. B. Hubbard and P. G. Wolynes, J. Chem. Phys. **69**, 998 (1978).
[22] H. J. Bakker, Chem. Rev. **108**, 1456 (2008); A. W. Omta, M. F. Kropman, S. Woutersen, and H. J. Bakker, Science **301**, 347 (2003); D. E. Moilanen, E. E. Fenn, Y. S. Lin, J. L. Skinner, B. Bagchi, and M. D. Fayer, Proc. Natl. Acad. Sci. U.S.A. **105**, 5295 (2008); H. S. Tan, I. R. Piletic, and M. D. Fayer, J. Chem. Phys. **122**, 174501 (2005).
[23] M. B. Ji and K. J. Gaffney, J. Chem. Phys. **134**, 044516 (2011); M. B. Ji, M. Odelius, and K. J. Gaffney, Science **328**, 1003 (2010); S. Park, M. Odelius, and K. J. Gaffney, J. Phys. Chem. B **113**, 7825 (2009).
[24] K. J. Gaffney, M. B. Ji, M. Odelius, S. Park, and Z. Sun, Chem. Phys. Lett. **504**, 1 (2011).
[25] D. Paoli, M. Lucon, and M. Chabanel, Spectrochim. Acta A **34**, 1087 (1978).
[26] M. Chabanel and Z. Wang, J. Phys. Chem. **88**, 1441 (1984); M. Chabanel, M. Lucon, and D. Paoli, J. Phys. Chem. **85**, 1058 (1981).
[27] J. Barthel, R. Buchner, and E. Wismeth, J. Solution Chem. **29**, 937 (2000).
[28] M. B. Ji, S. Park, and K. J. Gaffney, J. Phys. Chem. Lett. **1**, 1771 (2010).
[29] S. Park, M. B. Ji, and K. J. Gaffney, J. Phys. Chem. B **114**, 6693 (2010).
[30] K. Ohta and K. Tominaga, Chem. Phys. Lett. **429**, 136 (2006); M. Li, J. Owrutsky, M. Sarisky, J. P. Culver, A. Yodh, and R. M. Hochstrasser, J. Chem. Phys. **98**, 5499 (1993); V. Lenchenkov, C. X. She, and T. Q. Lian, J. Phys. Chem. B **110**, 19990 (2006);K. Dahl, G. M. Sando, D. M. Fox, T. E. Sutto, and J. C. Owrutsky, J. Chem. Phys. **123** (2005).
[31] M. B. Ji, R. W. Hartsock, Z. Sun, and K. J. Gaffney, J. Phys. Chem. B **115**, 11399 (2011).
[32] C. F. Guerra, J. G. Snijders, G. te Velde, and E. J. Baerends, Theor. Chem. Acc. **99**, 391 (1998); G. T. Velde, F. M. Bickelhaupt, E. J. Baerends, C. F. Guerra, S. J. A. Van Gisbergen, J. G. Snijders, and T. Ziegler, J. Comput. Chem. **22**, 931 (2001).
[33] M. Chabanel, Pure Appl. Chem. **62**, 35 (1990).
[34] P. Goralski and M. Chabanel, Inorg. Chem. **26**, 2169 (1987).
[35] D. Paoli, M. Lucon, and M. Chabanel, Spectrochim. Acta, Part A **35**, 593 (1979).
[36] J. Vaes, M. Chabanel, and M. L. Martin, J. Phys. Chem. **82**, 2420 (1978).
[37] P. W. Schultz, G. E. Leroi, and J. F. Harrison, Mol. Phys. **88**, 217 (1996).
[38] O. Squalli, M. C. M. Costa, A. Cartier, and M. Chabanel, J. Mol. Struct.: THEOCHEM **109**, 11 (1994).

[39]T. J. Chuang and K. B. Eisenthal, J. Chem. Phys. **57**, 5094 (1972); B. J. Berne and R. Pecora, *Dynamic Light Scattering* (Dover, Mineola, 2000).
[40]J. T. Edward, J. Chem. Educ. **47**, 261 (1970).
[41]M. A. Berg, J. Chem. Phys. **132**, 144105 (2010); M. A. Berg, J. Chem. Phys. **132**, 144106 (2010); K. M. Gaab and C. J. Bardeen, J. Phys. Chem. A **108**, 10801 (2004); K. M. Gaab and C. J. Bardeen, Phys. Rev. Lett. **93**, 056001 (2004); S. Garrett-Roe and P. Hamm, Acc. Chem. Res. **42**, 1412 (2009); S. Garrett-Roe, F. Perakis, F. Rao, and P. Hamm, J. Phys. Chem. B **115**, 6976 (2011); C. Khurmi and M. A. Berg, J. Phys. Chem. A **112**, 3364 (2008); E. van Veldhoven, C. Khurmi, X. Z. Zhang, and M. A. Berg, ChemPhysChem **8**, 1761 (2007).
[42]See supplementary material at http://dx.doi.org/10.1063/1.3665140 for discussion of vibrational peak assignments, LiNCS concentration dependent FTIR spectra, and anisotropy measurements in dimethyl carbonate and ethyl acetate.